JOURNAL OF COMPUTATIONAL PHYSICS 106, 299–305 (1993)

A Semi-implicit Spectral Method for the Anelastic Equations

SCOTT R. FULTON

Department of Mathematics and Computer Science, Clarkson University, Potsdam, New York 13699-5815

Received October 16, 1991

This paper describes the efficient and accurate solution of the two-dimensional anelastic equations by a Fourier–Chebyshev spectral method. A fourth-order Runge–Kutta method is used for the time integration, with the diffusion terms treated implicitly and all other terms (including the pressure gradient) treated explicitly. The model is free from aliasing and converges quickly once the solution is resolved. Numerical results are given for nonlinear flow generated by an atmospheric density current.

1. INTRODUCTION

The need to solve nonlinear flow problems accurately has given rise to a large number of computational methods. A recent workshop at the National Center for Supercomputing Applications (NCSA) attempted to compare the performance of many such methods for a model problem involving nonlinear flow generated by an atmospheric density current [10, 11]. Most methods presented were based on finite differences or finite elements, which at best can converge only algebraically (e.g., second- or fourth-order accuracy in space).

In contrast, spectral methods approximate the solution of systems of partial differential equations by truncated series expansions using global basis functions. For periodic problems one uses trigonometric basis functions, while for limited domains without periodicity, Chebyshev polynomials are appropriate. In either case, the truncation error (for smooth solutions) decays exponentially once the solution is adequately resolved. Thus, when high accuracy is desired, spectral methods may be more efficient than finite difference or finite element methods. For a comprehensive introduction to spectral methods and their applications to fluid dynamics, see [1]. Applications of Chebyshev spectral methods to atmospheric models are discussed in [3, 4, 6].

This paper describes the efficient and accurate solution of the problem posed for the NCSA workshop by a spectral method. Section 2 presents the governing equations and boundary conditions. The spectral discretization described in Sections 3 and 4 is conventional (Fourier–Galerkin in x, Chebyshev–collocation in z), except for building symmetry into the Fourier expansions. However, the solution procedure described in Section 5 is simpler than that used in similar models based on the incompressible Navier–Stokes equations, e.g., [7; 1, Section 7.3], principally due to treating the pressure gradient terms explicitly. Also, the semi-implicit Runge–Kutta scheme used for the time integration gives higher-order accuracy in time than is customary in such calculations. The numerical results given in Section 6 demonstrate the accuracy and efficiency of the method and provide numerical evidence for exponential convergence.

2. GOVERNING EQUATIONS

The anelastic equations [8] for two-dimensional flow can be written in advective form as

$$u_t + uu_x + wu_z = -\frac{1}{\bar{\rho}} p_x + \nu \nabla^2 u, \tag{2.1a}$$

$$w_t + uw_x + ww_z = -\frac{1}{\bar{\rho}} p_z + \nu \nabla^2 w + \frac{g}{\bar{\theta}} (\theta - \bar{\theta}), \tag{2.1b}$$

$$\theta_t + u\theta_x + w\theta_z = \nu \nabla^2 \theta, \tag{2.1c}$$

$$(\bar{\rho} u)_x + (\bar{\rho} w)_z = 0, \tag{2.1d}$$

where $\nabla^2 = \partial^2/\partial x^2 + \partial^2/\partial z^2$. Here u and w are the velocity components in the x (horizontal) and z (vertical) directions, respectively, ρ is the density, p is the deviation pressure, $\theta = T[p_0/(\bar{p} + p)]^{\kappa}$ is the potential temperature, T is the absolute temperature, g is the acceleration due to gravity, and ν is the diffusion coefficient. The basic state variables (denoted by overbars) depend only on z and are defined by

$$\bar{T}(z) = T_0 - \frac{gz}{c_p}, \tag{2.2a}$$

$$\bar{p}(z) = p_0 \left(\frac{\bar{T}}{T_0} \right)^{1/\kappa}, \tag{2.2b}$$

0021-9991/93 $5.00

$$\bar{\rho}(z) = \frac{\bar{p}}{R_d \bar{T}}, \tag{2.2c}$$

$$\bar{\theta}(z) = T_0, \tag{2.2d}$$

where $\kappa = R_d/c_p$ (where R_d and c_p are the gas constant and the specific heat at constant pressure for dry air) and T_0 and p_0 are constant reference values. The pressure p in (2.1) is the deviation from $\bar{p}$ (the total pressure is $\bar{p} + p$); it satisfies the diagnostic equation

$$\nabla^2 p = (\bar{\rho}F)_x + (\bar{\rho}G)_z, \tag{2.3}$$

where

$$F = \nu \nabla^2 u - (uu_x + wu_z) \tag{2.4a}$$

and

$$G = \nu \nabla^2 w - (uw_x + ww_z) + \frac{g}{\bar{\theta}}(\theta - \bar{\theta}). \tag{2.4b}$$

The computational domain is the rectangle $0 \leqslant x \leqslant L$, $0 \leqslant z \leqslant H$, with boundary conditions

$$u = w_x = \theta_x = 0 \quad \text{at} \quad x = 0, \quad x = L \tag{2.5a}$$

and

$$u_z = w = \theta_z = 0 \quad \text{at} \quad z = 0, \quad z = H. \tag{2.5b}$$

Making these substitutions into (2.1a), (2.1b) and using (2.4) gives

$$p_x = \bar{\rho}F \quad \text{at} \quad x = 0, \quad x = L \tag{2.6a}$$

and

$$p_z = \bar{\rho}G \quad \text{at} \quad z = 0, \quad z = H \tag{2.6b}$$

as boundary conditions for the pressure equation (2.3).

3. FOURIER METHOD IN x

In view of the boundary conditions (2.5a), we can extend the x-domain to $-L \leqslant x \leqslant L$ by symmetry (with u odd and w, θ, and p even functions of x), and then assume all variables are periodic in x with period $2L$. This allows us to represent the variables by truncated Fourier series expansions in x; note that this would not be appropriate if the problem to be studied truly had walls at the lateral boundaries, as implied by (2.5a), but for the symmetric problem to be studied [cf. Section 6] the two approaches are equivalent. To build in the symmetry, we define the basis functions

$$c_k = \cos\left(\frac{k\pi x}{L}\right), \qquad s_k = \sin\left(\frac{k\pi x}{L}\right), \tag{3.1}$$

and we approximate the model variables by

$$u(x, z, t) = \sum_{k=1}^{N_x} u_k(z, t)\, s_k(x), \tag{3.2a}$$

$$w(x, z, t) = \sum_{k=0}^{N_x} \frac{1}{\gamma_k} w_k(z, t)\, c_k(x), \tag{3.2b}$$

$$\theta(x, z, t) = \sum_{k=0}^{N_x} \frac{1}{\gamma_k} \theta_k(z, t)\, c_k(x), \tag{3.2c}$$

$$p(x, z, t) = \sum_{k=0}^{N_x} \frac{1}{\gamma_k} p_k(z, t)\, c_k(x), \tag{3.2d}$$

where $\gamma_0 = 2$ and $\gamma_k = 1$ for $k > 0$. With respect to the inner product

$$(f, g) = \frac{2}{L}\int_0^L f(x)\, g(x)\, dx \tag{3.3}$$

the basis functions (3.1) have the orthogonality properties

$$(c_j, c_k) = \begin{cases} \gamma_k, & \text{if } j = k; \\ 0, & \text{otherwise;} \end{cases} \tag{3.4a}$$

$$(s_j, s_k) = \begin{cases} 1, & \text{if } j = k > 0; \\ 0, & \text{otherwise;} \end{cases} \tag{3.4b}$$

so the coefficients in (3.2) are given by

$$u_k = (u, s_k) \qquad (k = 1, \ldots, N_x), \tag{3.5a}$$

$$w_k = (w, c_k) \qquad (k = 0, \ldots, N_x), \tag{3.5b}$$

$$\theta_k = (\theta, c_k) \qquad (k = 0, \ldots, N_x), \tag{3.5c}$$

$$p_k = (p, c_k) \qquad (k = 0, \ldots, N_x). \tag{3.5d}$$

To derive the Galerkin approximation to (2.1) we take the inner product (3.3) of (2.1a) with s_k and (2.1b)–(2.1d) with c_k and use (3.2) and (3.4) to obtain

$$\frac{\partial u_k}{\partial t} + (uu_x + wu_z, s_k) = -\frac{1}{\bar{\rho}}(-\bar{k}p_k) + \nu\left(\frac{\partial^2 u_k}{\partial z^2} - \bar{k}^2 u_k\right), \tag{3.6a}$$

$$\frac{\partial w_k}{\partial t} + (uw_x + ww_z, c_k) = -\frac{1}{\bar{\rho}}\frac{\partial p_k}{\partial z} + \nu\left(\frac{\partial^2 w_k}{\partial z^2} - \bar{k}^2 w_k\right) + \frac{g}{\bar{\theta}}(\theta_k - 2\bar{\theta}\delta_{0k}), \tag{3.6b}$$

$$\frac{\partial \theta_k}{\partial t} + (u\theta_x + w\theta_z, c_k) = \nu\left(\frac{\partial^2 \theta_k}{\partial z^2} - \bar{k}^2 \theta_k\right), \tag{3.6c}$$

$$\bar{k}\bar{\rho} u_k + \frac{\partial(\bar{\rho} w_k)}{\partial z} = 0, \tag{3.6d}$$

where $\bar{k} = k\pi/L$ and δ_{jk} is the Kronecker delta. Likewise, the Galerkin analogue of (2.3) is

$$-\bar{k}^2 p_k + \frac{\partial^2 p_k}{\partial z^2} = \bar{k}\bar{\rho} F_k + \frac{\partial}{\partial z}(\bar{\rho} G_k), \tag{3.7}$$

where $F_k = (F, s_k)$ and $G_k = (G, c_k)$, and the boundary conditions (2.6b) become

$$\frac{\partial p_k}{\partial z} = \bar{\rho} G_k \qquad \text{at} \quad z = 0, \quad z = H. \tag{3.8}$$

To compute the nonlinear terms in (3.6) we use the transform method [9]. For example, consider the calculation of

$$W_k = (UV, c_k), \tag{3.9}$$

where U and V are any two even model variables and $W = UV$ is their product (the odd/sine case is similar). We start with the coefficients of U and V satisfying

$$\begin{aligned} U(x) &= \sum_{k=0}^{N_x} \frac{1}{\gamma_k} U_k c_k(x), \\ V(x) &= \sum_{k=0}^{N_x} \frac{1}{\gamma_k} V_k c_k(x) \end{aligned} \tag{3.10}$$

and pad them with zeros out to $k = M_x > N_x$, e.g.,

$$\tilde{U}_k = \begin{cases} U_k, & 0 \leqslant k \leqslant N_x; \\ 0, & N_x < k \leqslant M_x. \end{cases} \tag{3.11}$$

We then evaluate U and V at the transform gridpoints $x_j = jL/M_x$ via discrete cosine transforms, e.g.,

$$U_j = \sum_{k=0}^{M_x} \frac{1}{\tilde{\gamma}_k} \tilde{U}_k c_k(x_j), \qquad j = 0, ..., M_x, \tag{3.12}$$

where $\tilde{\gamma}_k = 2$ if $k = 0$ or $k = M_x$ and 1 otherwise (note that it is okay to divide the last term by two since it is in fact zero). We then multiply the values in physical space to obtain

$$W_j = U_j V_j, \qquad j = 0, ..., M_x, \tag{3.13}$$

and then transform back to obtain

$$\tilde{W}_k = \sum_{j=0}^{M_x} \frac{1}{\tilde{\gamma}_k} W_j c_k(x_j), \qquad k = 0, ..., M_x. \tag{3.14}$$

It can be shown [1, Section 3.2.2] that if $M_x > \frac{3}{2} N_x$ then $\tilde{W}_k = W_k$ for $k = 0, ..., N_x$; i.e., the nonlinear term is computed without aliasing.

4. CHEBYSHEV METHOD IN z

In view of the rigid vertical boundaries implied by (2.5b), Fourier expansions in z would be inappropriate, giving only algebraic convergence. Instead, we use Chebyshev expansions, which give exponential convergence (to smooth solutions) independent of the boundary conditions [5]. Formally, for any model variable U which depends on z (e.g., u_k, w_k, θ_k, or p_k) we write

$$U(z) = \sum_{n=0}^{M_z} \hat{U}_n T_n(z'), \tag{4.1}$$

where $T_n(z') = \cos[n \cos^{-1}(z')]$ is the Chebyshev polynomial of degree n and $z' = -1 + 2z/H$. We relate these expansions to the model equations by the collocation projection; i.e., we require (3.6) to hold exactly at the Chebyshev collocation points

$$\bar{z}_j = \frac{H}{2}(1 + \bar{z}'_j), \quad \bar{z}'_j = \cos(j\pi/M_z), \quad j = 0, ..., M_z, \tag{4.2}$$

when the variables are all replaced by truncated Chebyshev series of the form (4.1). The Dirichlet conditions on w simply replace the collocation equations for w at $z = 0$ and $z = H$, while the treatment of the Neumann conditions on u, θ, and p will be described below.

In practice, each model variable U is represented by its values $\bar{U}_j = U(\bar{z}_j)$ at the collocation points in z, and its Chebyshev spectral coefficients $\hat{U}_n$ come into play in only two ways. First, to evaluate the z-derivative of U at the collocation points, we transform U to Chebyshev spectral space via

$$\hat{U}_n = \frac{2}{M_z \bar{\gamma}_n} \sum_{j=0}^{M_z} \frac{1}{\bar{\gamma}_j} \bar{U}_j T_n(\bar{z}'_j) \tag{4.3}$$

(where $\bar{\gamma}_n = 2$ if $n = 0$ or $n = M_z$ and 1 otherwise), compute the coefficients $\hat{U}^{(1)}_n$ of U_z via the backward recurrence relation

$$\gamma_{n-1} \hat{U}^{(1)}_{n-1} - \hat{U}^{(1)}_{n+1} = \frac{4n}{H} \hat{U}_n, \tag{4.4}$$

where $\hat{U}^{(1)}_{M_z} = \hat{U}^{(1)}_{M_z+1} = 0$, and transform the result back to physical space to obtain the values

$$\bar{U}^{(1)}_j = U_z(\bar{z}_j) = \sum_{n=0}^{M_z} \hat{U}^{(1)}_n T_n(\bar{z}'_j). \tag{4.5}$$

Second, to solve a problem of the form

$$\lambda^2 U - U_{zz} = V, \qquad 0 < z < H, \tag{4.6}$$

where λ is a constant and V is a known function of z (e.g., (3.7)), we transform it to obtain

$$\lambda^2 \hat{U}_n - \hat{U}^{(2)}_n = \hat{V}_n, \qquad n = 0, \ldots, M_z - 2, \tag{4.7}$$

where $\hat{U}^{(2)}_n$ is the coefficient of U_{zz}. We then solve (4.7), together with two equations arising from either Dirichlet or Neumann boundary conditions, by converting it to a pair of diagonally dominant tridiagonal linear systems [5, Section 10], and transform the results back to obtain U. In both cases, working in spectral space has the advantage of speed: the direct operations would involve full matrices and thus require $(O(M_z^2)$ operations, whereas computing (4.4) and solving (4.7) each require only $O(M_z)$ operations. The transforms (4.3) and (4.5) require only $O(M_z \log M_z)$ operations since they can be computed as discrete cosine transforms using the FFT algorithm.

The Chebyshev collocation method as described above is actually a pseudospectral method, in that it includes aliasing. However, filtering the Chebyshev spectral coefficients by retaining only the modes $0 \leqslant n \leqslant N_z$, where $\frac{3}{2}N_z < M_z$, removes the aliasing and results in a true spectral method. In practice, this is easily accomplished in the course of solving implicit problems of the form (4.7) at each time step as described below.

5. TIME INTEGRATION

The classical fourth-order Runge–Kutta (RK4) scheme is often practical for Chebyshev spectral models [3]: it is easy to implement, sufficiently accurate, and conditionally stable (unlike the leapfrog scheme, which for Chebyshev models is unconditionally unstable). However, the time step required for stability may be excessively small. In this model, the advection terms force $\Delta t = O(N_z^{-2})$ and the diffusion terms force $\Delta t = O(N_z^{-4})$, so for large N_z, it is advantageous to treat at least the diffusion terms implicitly.

To formulate a semi-implicit RK4 method, it is convenient to think of the present space-discretized model as a special case of a generic time-dependent model described by predictive equations of the form

$$\frac{\partial \mathbf{v}(t)}{\partial t} = A(t, \mathbf{v}, \mathbf{w}) + B(t, \mathbf{v}, \mathbf{w}) \tag{5.1a}$$

and diagnostic equations of the form

$$C(t, \mathbf{v}, \mathbf{w}) = 0. \tag{5.1b}$$

Here $\mathbf{v}(t)$ and $\mathbf{w}(t)$ are vectors consisting of the predicted and diagnosed model variables, respectively; the terms A and B are to be treated implicitly and explicitly, respectively. Using backward differencing for A and the RK4 method for B gives a one-step time integration scheme, in which each step consists of four stages (or partial steps) as follows:

$$\frac{\tilde{\mathbf{v}}^{l+1/2} - \mathbf{v}^l}{\Delta t/2} = \tilde{A}^{l+1/2} + B^l, \qquad \tilde{C}^{l+1/2} = 0, \tag{5.2a}$$

$$\frac{\mathbf{v}^{l+1/2} - \mathbf{v}^l}{\Delta t/2} = A^{l+1/2} + \tilde{B}^{l+1/2}, \qquad C^{l+1/2} = 0, \tag{5.2b}$$

$$\frac{\tilde{\mathbf{v}}^{l+1} - \mathbf{v}^l}{\Delta t} = \tilde{A}^{l+1} + B^{l+1/2}, \qquad \tilde{C}^{l+1} = 0, \tag{5.2c}$$

$$\frac{\mathbf{v}^{l+1} - \mathbf{v}^l}{\Delta t} = A^{l+1} + \bar{B}^{l+1}, \qquad C^{l+1} = 0. \tag{5.2d}$$

Here l specifies the time level $t_l = l\,\Delta t$ and the A, B, and C terms are evaluated as $A^{l+1} = A(t_{l+1}, \mathbf{v}^{l+1}, \mathbf{w}^{l+1})$, $B^l = B(t_l, \mathbf{v}^l, \mathbf{w}^l)$, $\tilde{C}^{l+1/2} = C(t_{l+1/2}, \tilde{\mathbf{v}}^{l+1/2}, \tilde{\mathbf{w}}^{l+1/2})$, etc.; the one exception to this general notation is

$$\bar{B}^{l+1} = \tfrac{1}{6}(B^l + 2\tilde{B}^{l+1/2} + 2B^{l+1/2} + \tilde{B}^{l+1}). \tag{5.3}$$

Note that each stage involves solving an implicit problem of the form

$$\mathbf{v}^{l+\beta} - \gamma A^{l+\beta} = \text{known terms}, \qquad C^{l+\beta} = 0 \tag{5.4}$$

for $\mathbf{v}^{l+\beta}$ and $\mathbf{w}^{l+\beta}$, where β and γ are constants.

For the present model, $\mathbf{v}(t)$ and $\mathbf{w}(t)$ consist of the model variables u, w, θ (in Fourier spectral space in x and at Chebyshev collocation points in z), and A represents the diffusion terms and B all others (advection, pressure gradient, and buoyancy). The diagnostic condition C here represents the boundary conditions in z; the pressure p enters only in computing the pressure gradient terms in B. We execute each of the four stages of the scheme (5.2) as follows:

1. Given u, w, θ at the beginning of the stage, compute the explicit terms B:
   a. compute the advection and buoyancy terms
   b. solve the pressure equation (3.7) for p
   c. compute the pressure gradient terms.
2. Solve the implicit problem (5.4) for u, w, θ at the end of the stage: the problem for u takes the form

$$u_k - \gamma\nu\left(\bar{k}^2 u_k - \frac{\partial^2 u_k}{\partial z^2}\right) = \text{known terms}, \tag{5.5}$$

where the boundary conditions $\partial u_k/\partial z = 0$ are applied at $z = 0$ and $z = H$; the problems for w and θ are analogous.

Note that (3.7) and (5.5) have the same form as (4.7) and thus can be solved efficiently in Chebyshev spectral space as described in Section 4. Also, we could predict only w and θ and diagnose u from continuity, but imposing the Neumann boundary conditions on u is more awkward and the savings in computer time and storage are minimal.

6. RESULTS

The initial condition for the NCSA workshop problem consists of a negatively buoyant blob of air of absolute temperature $T = \bar{T} + \Delta T$, with

$$\Delta T = \begin{cases} -\frac{1}{2}T_1\,[\cos(\pi l) + 1], & \text{if } l < 1, \\ 0, & \text{if } l \geqslant 1, \end{cases} \tag{6.1a}$$

where

$$l = \left[\left(\frac{x - x_c}{x_r}\right)^2 + \left(\frac{z - z_c}{z_r}\right)^2\right]^{1/2}. \tag{6.1b}$$

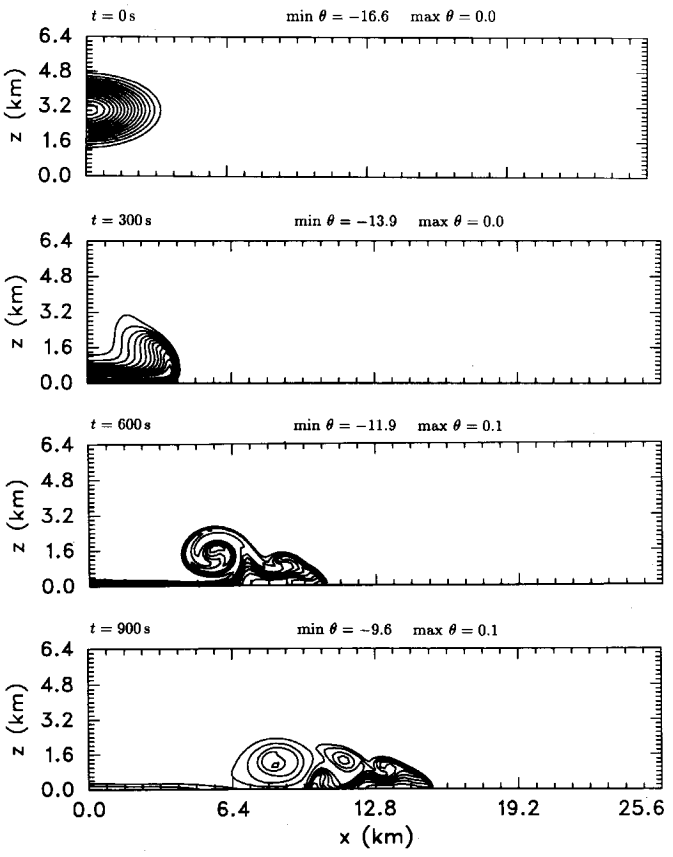

FIG. 1. Reference solution ($M_x = 512$) deviation $\theta_{\text{ref}} - \bar{\theta}$ vs x and z.

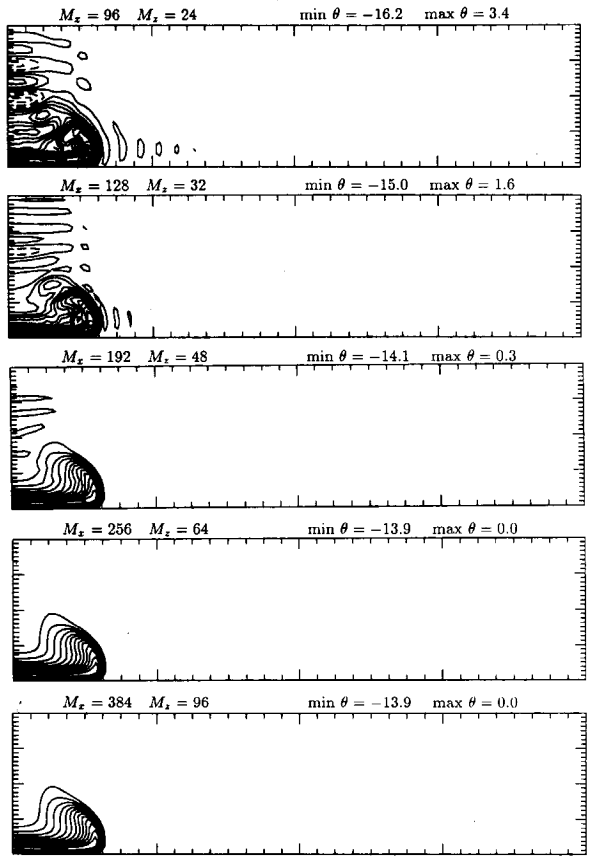

FIG. 2. Deviation θ vs. x and z at $t = 300$ s.

The corresponding potential temperature is $\theta = T(p_0/\bar{p})^{\kappa}$, and the initial u and w fields are zero. The constants used are $R_d = 287.04$, $c_p = 1004$, $p_0 = 10^5$, $T_0 = 300$, $g = 9.81$, $\nu = 75$, $L = 25600$, $H = 6400$, $x_c = 0$, $x_r = 4000$, $z_c = 3000$, $z_r = 2000$, and $T_1 = 15$, all in SI units. For all model runs the spatial resolution was specified by M_x, with $M_z = M_x/4$ and N_x and N_z chosen as large as possible while still avoiding aliasing (i.e., $N_x < \frac{3}{2}M_x$ and $N_z < \frac{3}{2}M_z$; see also Table I).

Figure 1 shows the deviation θ field (i.e., $\theta - \bar{\theta}$) for a high-resolution reference run ($M_x = 512$). The convergence of the model is demonstrated by the solutions shown in Figs. 2–4

TABLE I

Execution Time on a CRAY Y-MP4/464 (for $\Delta t = 2$ s)

M_x	M_z	N_x	N_z	h (m)	CPU seconds
64	16	42	10	400	11
96	24	63	15	267	19
128	32	85	21	200	31
192	48	127	31	133	62
256	64	170	42	100	116
384	96	255	63	67	247
512	128	341	85	50	453

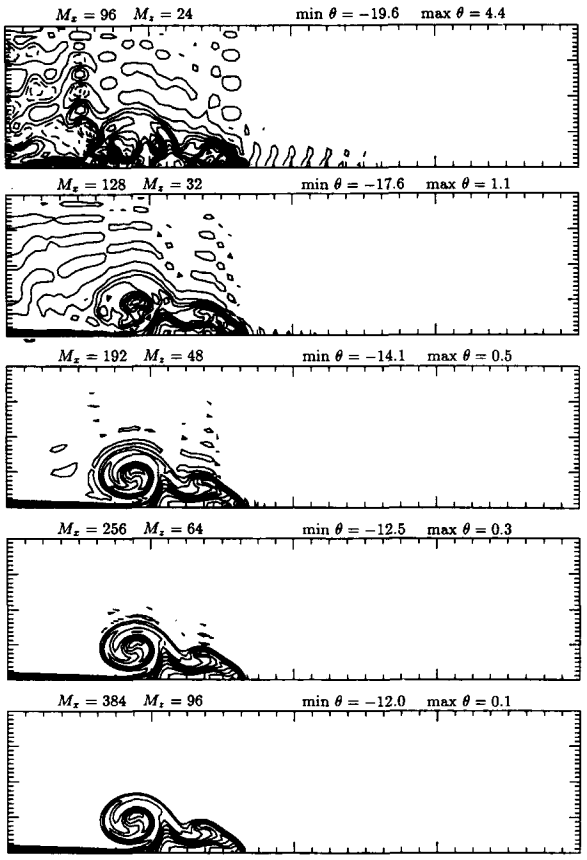

FIG. 3. Deviation θ vs. x and z at $t = 600$ s.

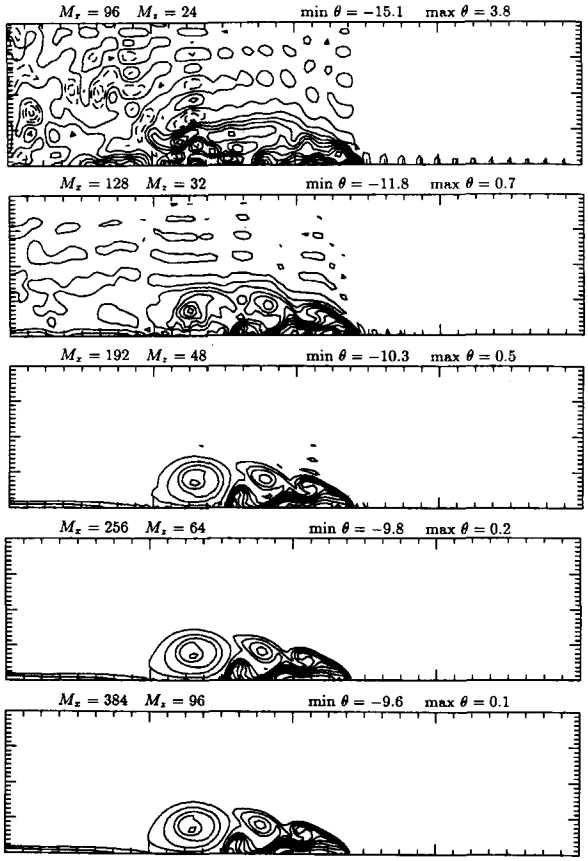

FIG. 4. Deviation θ vs. x and z at $t = 900$ s.

for various spatial resolutions. To quantify the rate of convergence (or more properly, the rate of self-convergence), we compare the solution for θ at various resolutions to the solution θ_{ref} from the reference run ($M_x = 512$). Figure 5 shows this difference measured in the l_2 norm

$$\|\theta - \theta_{\text{ref}}\|_2 = \left\{ \frac{1}{IJ} \sum_{i=0}^{I} \sum_{j=0}^{J} [\theta(x_i, z_j) - \theta_{\text{ref}}(x_i, z_j)]^2 \right\}^{1/2}, \tag{6.2a}$$

and Fig. 6 shows the same quantity measured in the l_∞ norm

$$\|\theta - \theta_{\text{ref}}\|_\infty = \max_{0 \leqslant i \leqslant I,\, 0 \leqslant j \leqslant J} |\theta(x_i, z_j) - \theta_{\text{ref}}(x_i, z_j)|. \tag{6.2b}$$

Here $x_i = iL/I$ and $z_j = jH/J$ with $I = 256$ and $J = 64$; i.e., the solution is evaluated on a uniform grid with mesh size $h = 100$ m (this same grid was used to produce Figs. 1–4). We see that at $t = 0$ the convergence is somewhat slow, as might be expected, since the initial condition (6.1) is not infinitely differentiable. At later times the convergence appears to be exponential: the error is proportional to e^{-M_x/M_0}, with M_0 in the range 40–70. Results of numerical sensitivity studies (not shown) indicate that the model is stable with respect to small perturbations of the initial conditions.

The above results were all produced using the time step $\Delta t = 2$s, which is stable for resolutions to at least $M_x = 512$. Comparison with runs at smaller time steps indicate that the time discretization error is considerably smaller than the space discretization error to about $M_x = 256$, so in fact larger time steps could be used without loss of accuracy. At $M_x = 384$, the time discretization error at $\Delta t = 2$s is probably about four times as great as the space discretization error. The solution converges slowly with decreasing Δt at these higher resolutions; the dominant contribution to the error appears to be from the diffusion terms, which are treated with only a first-order method in time. If higher accuracy were desired, one could use a higher-order implicit method for the diffusion terms. However, treating them explicitly (e.g., with the RK4 scheme) is probably not practical: with $M_x = 256$, the fully explicit RK4 scheme already requires $\Delta t \leqslant 0.5$ s for stability, and Δt decreases like M_x^{-4} due to the diffusion terms.

The model was coded in FORTRAN 77; all significant calculations are easily vectorizable. All sine, cosine, and Chebyshev transforms were computed by converting them

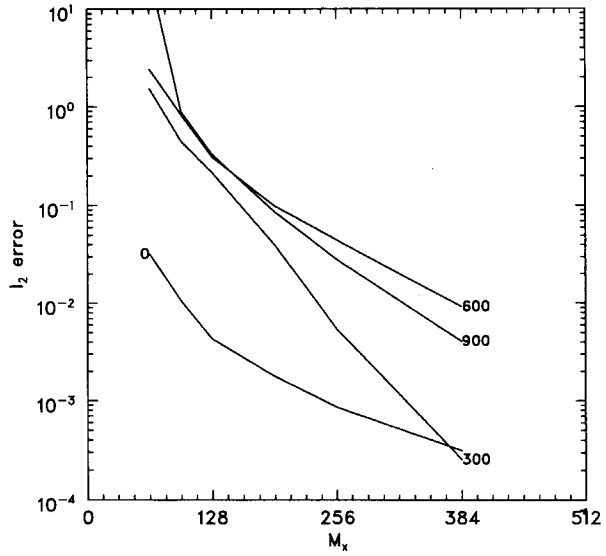

FIG. 5. Error in θ (difference from $M_x = 512$ solution) measured in the l_2 norm as a function of M_x for $t = 0$, 300, 600, and 900 s as labeled.

to half-complex to real discrete Fourier transforms by the method of [2] and evaluating those by the Temperton FFT routines [12]. (A bug in the assembly-language version of these routines (ecmfft) gave nondeterministic results, so an all-FORTRAN version (about 25% slower) was used.) Table I shows the execution time for the model on the CRAY Y-MP4/464 at NCSA for $\Delta t = 2$ s with various spatial resolutions (here $h = L/M_x$ gives the mesh spacing in x on the transform grid). Most of the work seems tied up in the computation of the nonlinear terms; neither predicting only w and θ or using the fully explicit RK4 scheme (with the same time step) makes any significant change in the execution time.

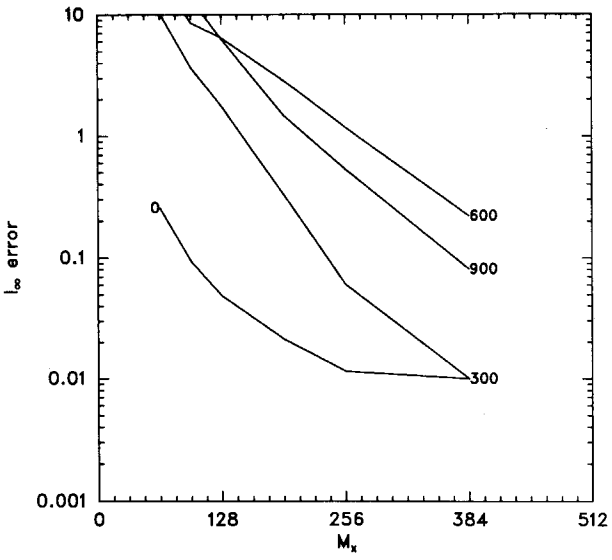

FIG. 6. Error in θ (difference from $M_x = 512$ solution) measured in the l_∞ norm as a function of M_x for $t = 0$, 300, 600, and 900 s as labeled.

7. CONCLUDING REMARKS

The spectral model described here solves the NCSA workshop problem accurately in a reasonable amount of computer time. It is free from aliasing and converges quickly once the solution is adequately resolved. Semi-implicit time differencing allows reasonable sized time steps to be used. If extremely high accuracy were desired, one should use a higher-order time scheme for the diffusion terms, since they limit the accuracy at high resolutions. However, the present model can compute the solution for θ everywhere to within better than 0.1 K, and it is doubtful that higher accuracy would normally be needed.

ACKNOWLEDGMENTS

This work was partially supported by the National Science Foundation under Grant ATM-8918725, and computer time was provided by the National Center for Supercomputing Applications, University of Illinois at Urbana-Champaign.

REFERENCES

1. C. Canuto, M. Y. Hussaini, A. Quarteroni, and T. A. Zang, *Spectral Methods in Fluid Dynamics* (Springer-Verlag, New York, 1988).
2. J. W. Cooley, P. A. W. Lewis, and P. D. Welch, *J. Sound Vib.* **12**, 315 (1970).
3. S. R. Fulton and W. H. Schubert, *Mon. Weather Rev.* **115**, 1940 (1987).
4. S. R. Fulton and W. H. Schubert, *Mon. Weather Rev.* **115**, 1954 (1987).
5. D. Gottlieb and S. A. Orszag, *Numerical Analysis of Spectral Methods* (Soc. Ind. and Appl. Math., Philadelphia, 1977).
6. H. C. Kuo and W. H. Schubert, *Q. J. R. Meteorol. Soc.* **114**, 887 (1988).
7. P. Moin and J. Kim, *J. Comput. Phys.* **35**, 381 (1980).
8. Y. Ogura and N. A. Phillips, *J. Atmos. Sci.* **19**, 173 (1962).
9. S. A. Orszag, *J. Atmos. Sci.* **27**, 890 (1970).
10. J. M. Straka, R. B. Wilhelmson, L. J. Wicker, J. R. Anderson, and K. K. Droegemeier (Preprints, Ninth Conference on Numerical Weather Prediction, American Meteorological Society, Denver, Colorado, October 14–18, 1991).
11. J. M. Straka, R. B. Wilhelmson, L. J. Wicker, J. R. Anderson, and K. K. Droegemeier, *Int. J. Numer. Methods Fluids.*, to appear.
12. C. Temperton, *J. Comput. Phys.* **52**, 1 (1983).